Methods of Improving the Performance of Light-Emitting Electrochemical Cells Based on the $Ru(bpy)_3$ Complex

by

Whitney Gaynor

Submitted to the Department of Materials Science and Engineering in Partial Fulfillment of the Requirements for the Degree of

Bachelor of Science

at the

Massachusetts Institute of Technology

June 2004

Signature of Author .....
Department of Materials Science and Engineering
May 12, 2004

Certified by.....
Michael F. Rubner
TDK Professor of Materials Science and Engineering
Thesis Supervisor

Accepted by.....
Lorna Gibson
Chair, Undergraduate Thesis Committee

Table of Contents

Acknowledgements

All work in this thesis was done in collaboration with Nobuaki Takane of Hitachi Chemical Company in Japan. I'd like to thank Nobuaki for his support and for sharing his ideas with me. I'd also like to thank the entire Rubner group at MIT, especially Mike Berg for help with the fluorescent dye, Koji Itano for donating SPS/PAH films, and Professor Rubner for supporting the work and for all the help in putting this thesis together.

On a more personal note, I'd like to thank the Department of Materials Science at MIT, especially my academic advisor, Professor Adam Powell, for helping me choose the best path for me through college and into graduate school, and for helping to make my undergraduate experience successful. And last but not least, I'd like to thank the friends I've made through my four years at MIT, knowing full well that I would not have gotten through without you all.

1. Thesis Introduction

Organic light-emitting diodes (OLED's) have been touted as the next wave in display technology. They are attractive due to their potential for high efficiency, low loss, flat screen displays that can be produced in a cost-effective manner [1]. Transition metal complexes, such as ruthenium tris-bipyridine $Ru(bpy)_3^{2+}$ (Figure 1.1-a) which is studied here, are candidate materials for a class of organic light-emitting devices known as light-emitting electrochemical cells (LEC's). All of these devices utilize the same general concept and configuration. An active layer is sandwiched between a cathode and an anode. Figure 1.1-b shows a sandwich-style device configuration.

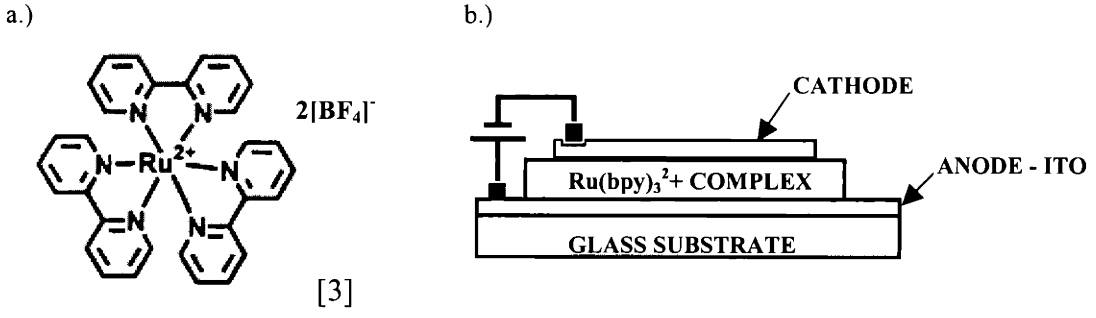

Figures 1.1a and b: The molecular structure of $Ru(bpy)_3[BF_4]_2$, and a sandwich-style device structure for an LEC based on the ruthenium complex.

The general behavior of organic LED's is a follows. A bias is applied that causes holes to be injected from the anode into the highest occupied molecular orbital (HOMO) of the organic active layer. These holes then migrate towards the center of the layer. Electrons are injected from the cathode into the lowest unoccupied molecular orbital (LUMO) of the organic active layer. They then move toward the center as well, combining with the holes to produce excitons. These excitons then recombine to produce photons, light

emission of a certain wavelength that is characteristic to the active layer [1]. Based on this mechanism, the active layer must be able to transport electrons and holes, and must have high luminescence efficiency.

The active layer in $Ru(bpy)_3^{2+}$ devices consists of a film of these molecules plus negatively charged counterions. In this study, BF_4^- was used. The current and capacitance characteristics of these devices show that an electrochemical junction is formed during operation [2]. When a forward bias is applied, the BF_4^- ions drift toward the ITO anode. This ion accumulation lowers the barrier for hole injection, and holes are injected into the HOMO of $Ru(bpy)_3^{2+}$, which is the t_{2g} orbital of the metal center. This produces a $Ru(bpy)_3^{3+}$ ion. As this occurs, the $Ru(bpy)_3^{2+}$ ions near the cathode enhance electron injection, injecting electrons into the LUMO of the molecule, which is the π^* orbital of the ligands to create an $Ru(bpy)_3^{+}$ ion. Steady state operation is achieved when the BF_4^- ions have completely redistributed themselves at an equilibrium distance from the electrodes, which is determined by the applied voltage. $Ru(bpy)_3$ ions are stable in these oxidized and reduced states, which is the reason that these devices are able to operate. Electrons and holes migrate toward each other by hopping between donor and acceptor sites [1]. When an electron from a $Ru(bpy)_3^{+}$ ion and a hole from an $Ru(bpy)_3^{3+}$ ion combine, they produce an excited state, $Ru(bpy)_3^{2+*}$, which decays into $Ru(bpy)_3^{2+}$, producing a photon. The mixed-valent states of the ions are conductive, and all the complexes are in electrochemical equilibrium [2]. The device exhibits no local charge neutrality, and Rudmann et al have reported that an electric field that increases in the center of the device must be present during its operation [2].

Ruthenium tris-bipyridine (and other transition metal complex) devices differ from other forms of OLED's and polymer LEC's. Unlike devices that behave as diodes, transition metal devices have a comparatively long turn-on time and exhibit no rectification. This turn-on time is an effect of the mobile counterion redistribution. Transition metal LEC's do not require low-work function metal cathodes because they are not limited by charge injection. Accumulation of ions at the contacts make the junctions behavior almost ohmic, while the turn-on voltage can be as low as the difference between the HOMO and LUMO of the active layer. As the applied voltage increases, the speed of the counterion redistribution increases, shortening the response time. As opposed to polymer LEC's, $Ru(bpy)_3$ devices are much more stable, as they do not suffer from phase separation between the polymer and the ions.

At the present time in the field, researchers seek to explore three aspects of the devices based on $Ru(bpy)_3^{2+}$: efficiency, response time, and device lifetime for practical applications. Many researchers have worked to improve the properties of these devices to ready them for applications such as monochromatic alphanumeric displays and backlights due to their low cost and simple fabrication of sandwich-style devices. Various aspects of these devices have been altered to improve their quality. The ligands on the complex themselves have been found to have an effect on device efficiency, and adding specific ligands to the $Ru(bpy)_3^{2+}$ ion improves both photoluminescent (PL) and electroluminescent (EL) efficiency [3]. Driving the devices using AC voltage at a 50% duty cycle improved the device lifetime by changing the counterion distribution during operation [4]. Blending the $Ru(bpy)_3^{2+}$ film with polymers improves the film quality, which increases the device lifetime [4]. Silver cathodes were found to be ideal in

increasing the device shelf-life, as Al cathodes exhibited degradation through chemical reactions with the active layer after long periods of time in the off state [5]. Experiments in which counterions were changed have been reported, with results showing that larger counterions produce devices with longer lifetimes and longer response times [3].

The experiments presented in this thesis build upon the previous work of the Rubner group and examine methods of improving $Ru(bpy)_3^{2+}$ device performance through blending with spin-cast polymer films and changing the device cathode structure. The properties of these new devices were measured and evaluated.

A method of combining $Ru(bpy)_3^{2+}$ salts with polyelectrolyte multilayer films to fabricate light-emitting devices was also investigated. This work aimed at a simple, water-based method of fabricating light-emitting devices over large areas. Ultimately, however, the performance properties of these devices could not compete with those of the spin-cast polymer blended films.

Polyelectrolyte multilayer films were developed by Decher et al. [6] in the early 1990's as an alternative to producing thin films using either the Langmuir-Blodgett technique or silane-SiO_2 or metal-phosphate self-assembled monolayers. This technique reliably produces higher quality films over larger areas than the previous techniques for nano-thickness film formation [6]. Currently, various sytems of polyelectrolyte multilayer films are under consideration as materials for a vast range of applications including biomaterials and drug delivery systems [7], anti-reflection coatings [8], photonic bandgap structures [9], nanoreactors [10] and templates for colloidal arrays [11] among others.

Films are formed through consecutive adsorption of polyelectrolytes onto a surface from aqueous solution [6]. The layers can be held together primarily through either ionic or hydrogen bonding [12,13], as was first shown by the Rubner group [14]. Figure 1.2 shows a schematic of the layer formation.

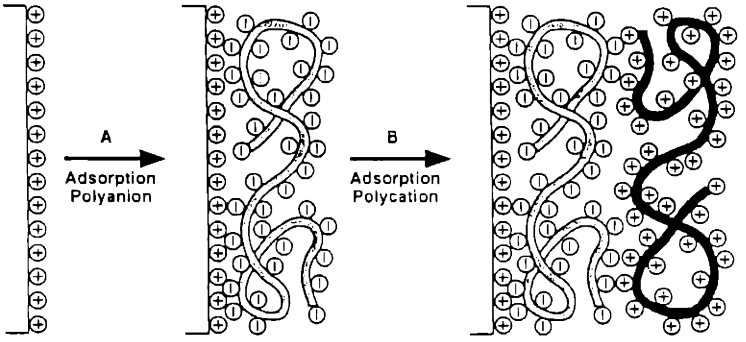

[6]

Figure 1.2: Schematic of the consecutive adsorption process that occurs in polyelectrolyte multilayer film formation

Electrostatic attractive forces draw polyelectrolyes from the solution and adhere them to the substrate, reversing the surface charge. This charge reversal serves to repel like charges and self-regulate the layer thickness and to facilitate the sequential adsorption of the next layer.

There are various factors that affect the formation of polyelectrolyte multilayer films. One is the pH of the polymer solutions prior to dipping the substrate. There is a threshold pH for each polymer at which film formation is possible due to the requirement of having enough charged species to adhere the molecule to both the previous layer and the succeeding layer in the film. When films do form, pH affects the morphology of the films, along with other important properties such as wetting contact angle [15]. For example, in films made from poly(acrylic acid) (PAA) and poly(allylamine

hydrochloride) (PAH) the bilayer thickness can range from 5 to 80 Å depending on the pH conditions of the solutions [15]. Another factor that affects film formation and properties is the ionic strength of the polymer solutions. Adding salt can also induce a threshold of film formation, as the salt ions pair with the charged segments of the polyions to prevent them from adhering to either a previous or subsequent layer [16]. Figure 1.3 shows a schematic of the effects of salt addition to polymer solutions in film formation. Salt affects the bilayer thickness, swelling, and water permeability of the films [16].

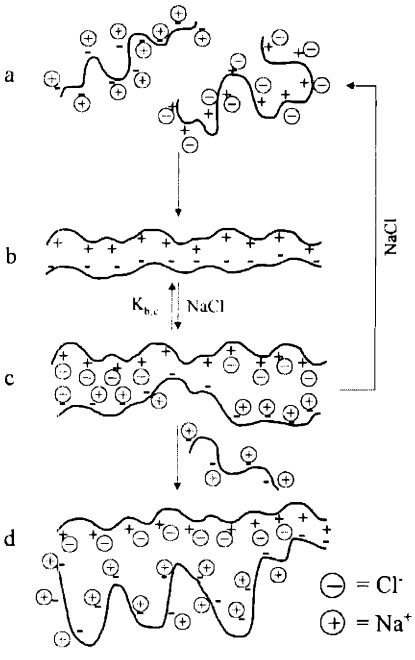

[16]

Figure 1.3: A schematic of the effect that salt has in polyelectrolyte multilayer formation and dissolution. In a. the ions are shown interacting with the charges on the polyions. Part b shows film formation, while parts c and d show swelling of the film and conformational changes that can occur due to charge shielding interactions with the salt ions.

As shown through salt studies, polyelectrolyte multilayer films are able to hold ions within their layers. These ions can be loaded into the films after formation as well. Ion loading and release characteristics can be affected by the pH of both the original polymer solutions as well as the solution in which the loading occurs [7].

Polyelectrolyte multilayer films, either in deposition or once on a substrate can be patterned on the micron scale using various techniques for applications such as colloid arrays [11]. Patterning can be done through polymer stamping [17] or inkjet printing [18,19]. The system explored in this paper can also be selectively etched using a commercial inkjet printer outfitted with low pH acid [8]. These patterned films can then be used in conjunction with $Ru(bpy)_3^{2+}$ light-emitting devices. The polyelectrolyte film acts as an insulator, blocking charge injection and thus emission in certain areas of the active layer. This allows for the creation of patterned light-emitting devices. This work also explored a novel method of etching polyelectrolyte mutlilayer films that can be easily used in conjunction with an inkjet printer.

Interactions between multilayer films fabricated from PAA at pH 3.5 and PAH at pH 7.5 and aqueous salt solutions of varying molarity and salt composition were examined. These films, due to the starting pH's of the respective polymer solutions form some of the thickest layers and roughest films of this particular polyion system, their bilayer thickness being in the range of 50-80 nm [20]. Etching effects on the nanometer scale were observed. Changes in film thickness could be observed on reflective silicon substrates as changes in reflected wavelengths and colors of light, creating a patternable color mirror. These types of mirrors could be useful in LCD display applications. These films also undergo a phase transformation by immersion in acidic baths to become micro- or nanoporous and function as antireflection coatings [8], giving this etching technique relevance to applications in optical communications.

References:

[1] Slinker, Bernards, Houston, Abruna, Bernhard, and Malliaras. "Solid-state electroluminescent devices based on transition metal complexes". *Chem. Commun.* 2003: 2392-2399.

[2] Rudmann, Shimada, and Rubner. "Operational mechanism of light-emitting devices based on Ru(II) complexes: Evidence for electrochemical junction formation". *J. Applied Physics.* 94,1: 115-122.

[3] Rudmann, Shimada, and Rubner. "Solid-State Light-Emitting Devices Based on the Tris-Chelated Ruthenium(II) Complex. 4. High-Efficiency Light-Emitting Devices Based on Derivatives of the Tris(2,2'-bipyridal) Ruthenium(II) Complex". *J. Am. Chem. Soc.* 124 (17): 4918-4921

[4] Rudmann and Rubner. "Single layer light-emitting devices with high efficiency and long lifetime based on tris(2,2' bipyridal) ruthenium(II) hexafluorophosphate". *J. of Applied Physics* 90 (9): 4338-4345. 2001

[5] Rudmann H, Shimada S, Rubner MF, Oblas DW, Whitten JE. "Prevention of the cathode induced electrochemical degradation of [Ru(bpy)(3)](PF6)(2) light emitting devices" J. Applied Phsyics 92 (3): 1576-1581. 2001

[6] Decher. "Fuzzy Nanoassemblies: Toward Layered Polymeric Multicomposites". *Science.* 277: 1232-1237.

[7] Chung and Rubner. "Methods of Loading and Releasing Low Molecular Weight Cationic Molecules in Weak Polyelectrolyte Multilayer Films". *Langmuir* 2002, 18: 1176-1183.

[8] Hiller J, Mendelsohn JD, Rubner MF. "Reversibly erasable nanoporous anti-reflection coatings from polyelectrolyte multilayers". *Nature Materials* 1 (1): 59-63. 2002

[9] Wang TC, Cohen RE, Rubner MF. "Polyelectrolyte multi layer-based photonic bandgap structures." *Abstr. Pap. Am. Chem. Soc.* 223: 275-POLY Part 2 APR 7 2002

[10] Wang TC, Rubner MF, Cohen RE. "Polyelectrolyte multilayer nanoreactors for preparing silver nanoparticle composites: Controlling metal concentration and nanoparticle size". *Langmuir* 18 (8): 3370-3375 APR 16 2002

[11] Zheng HP, Rubner MF, Hammond PT. "Particle assembly on patterned "plus/minus" polyelectrolyte surfaces via polymer-on-polymer stamping". *Langmuir.* 18 (11): 4505-4510. 2002

[12] Sukhishvili and Granick. "Layered, Erasable Polymer Multilayers Formed by Hydrogen-Bonded Sequential Self-Assembly". *Macromolecules* 2002, 35: 301-310.

[13] Wang, Fu, Wang, Fan, and Zhang. "Investigation into an Alternating Multilayer Film of Poly(4-Vinylpyridine) and Poly(acrylic acid) Based on Hydrogen Bonding". Langmuir, 1999. 15: 1360-1363.

[14] Stockton WB, Rubner MF. "Molecular-level processing of conjugated polymers .4. Layer-by-layer manipulation of polyaniline via hydrogen-bonding interactions" *Macromolecules*. 30 (9): 2717-2725. 1997

[15] Shiratori and Rubner. "pH-Dependent Thickness Behavior of Sequentially Adsorbed Layers of Weak Polyelectrolytes". *Macromolecules* 2000, 33: 4213-4219.

[16] Dubas and Schlenoff. "Polyelectrolyte Multilayers Containing a Weak Polyacid: Construction and Deconstruction" *Macromolecules* 2001, 34: 3736-3740.

[17] Berg MC, Choi J, Hammond PT, Rubner, MF. "Tailored micropatterns through weal: Polyelectrolyte stamping" *Langmuir.* 19 (6): 2231-2237. 2003

[18] Yang and Rubner. "Micropatterning of Polymer Thin Films with pH-Sensitive and Cross-linkable Hydrogen-Bonded Polyelectrolyte Multilayers". *J. Am. Chem. Soc.* 124, 10: 2100-2101. 2002.

[19] Yang, Mendelsohn, and Rubner. "New Class of Ultrathin, Highly Cell-Adhesion-Resistant Polyelectrolyte Multilayers with Micropatterning Capabilities". *Biomacromolecules* 2003 4: 987-994.

[20] Mendelsohn, Barrett, Chan, Pal, Mayes, and Rubner. "Fabrication of Microporous Thin Films from Polyelectrolyte Multilayers". Langmuir 2000. 16: 5017-5023

2. LEC's Based on Loading $Ru(bpy)_3^{2+}$ into Polyelectrolyte Multilayer Films

2.1. Chapter 2: Introduction

Light-emitting electrochemical cells fabricated from $Ru(bpy)_3^{2+}$ complexes have generated excitement in recent years due to their simple architecture, low operating voltage, and high external efficiencies [1]. Their operation is facilitated by motion of the counterions within the active layer of the device, enabling charge injection at the electrodes and exciton formation [1]. The prevailing method of processing the active layers in these devices is through spin-casting the films from organic solvent solutions [1-3]. This work explores an alternative method of fabricating these devices by combining them with polyelectrolyte multilayer films.

The goal of this work was to fabricate light-emitting electrochemical cells by loading salts containing $Ru(bpy)_3^{2+}$ and BF_4^- ions into polyelectrolyte multilayer films fabricated from poly(acrylic acid) (PAA) and poly(acrylamide) (PAAm). Previous work has been done both in fabricating ruthenium complex light-emitting devices in multilayer films [4] and in loading cationic molecules into polyelectrolyte multilayer films. The deprotonated carboxyl side groups in PAA bind to cations loaded into the film [5]. This work follows logically from these in loading the cationic $Ru(bpy)_3^{2+}$ into pre-fabricated film platforms.

Polyelectrolyte multilayer films prepared from PAA and PAAm are hydrophilic and held together through hydrogen-bonding [6]. They are made through a layer-by-layer dipping process into aqueous solutions of each polymer. The monomer repeat units of

each polymer are shown in Figure 2.1. Poly(acrylic acid), is a weak acid with a pK_a of about 6.5 [7]. Thus, to enable hydrogen-bonding within these layers, the pH of the polymer

Figure 2.1: Monomer repeat units of poly(acrylic acid) (PAA, left) and poly(acrylamide) (PAAm, right). Both contain groups that are able to undergo hydrogen bonding.

solutions must be kept very low during formation [6]. The fraction of ionized carboxyl groups are then available to bind to incoming $Ru(bpy)_3^{2+}$ ions. The films used in this work were fabricated from polymer solutions and rinse baths at pH 3.0. It has been shown that subjecting un-crosslinked samples to neutral pH baths, the film can be dissolved [6]. At low pH, these films can be formed reliably and relatively defect-free over large substrate areas. Thus, if this method of producing LEC's is successful, it would have advantages over current methods of processing. It would be suitable for large area coverage, and would be based on water instead of organic solvents.

2.2. Chapter 2: Experimental

PAA (pH 3.0)/PAAm (pH 3.0) films were fabricated onto 1"x1" glass substrates containing two strips of indium tin oxide (ITO). Substrates were cleaned using a sequence of detergent, de-ionized water, and isopropanol, all sonicated for 15 minutes

each. An HMS programmable slide stainer from Zeiss, Inc. was used to deposit the polymers onto the substrates. All polymer solutions and rinse baths were at pH 3.0. Poly(acrylic acid) (PAA) (MW = 90,000 in a 25% aqueous solution), poly(allylamine hydrochloride) (PAH) (MW = 70,000), and polyacrylamide (PAAm) (MW=10,000 in a 50% aqueous solution) were used in 10 mM aqueous solution. All films began with one layer of PAH followed by a set number of bilayers of PAA and PAAm. The slides were dipped into each polymer for 15 minutes, followed by three de-ionized water rinse baths for two minutes, one minute, and one minute before the next layer is added. The water used in these experiments was filtered through a Milli-Q academic system (Millipore Corporation) using a 0.22 μm Millistack filter at the outlet and a resistance higher than 18.2MΩ cm. After the films were complete, they were dried and cross-linked in vacuum at 140°C for three hours. Salt was then loaded into the film by dipping the substrate into a 10 mM aqueous solution for one minute, rinsing briefly in de-ionized water, and drying under compressed air. This process was followed by additional drying under vacuum at 180°C for two hours to remove the water. Previous research shows that the loading time after one minute does not affect the amount of salt absorbed by the polymer film.

The first films were deposited from pure polymer aqueous solutions and were loaded first with a $2x10^{-2}$M tetrabutyl ammonium tetrafluoroborate ($TBABF_4$) salt aqueous solution and then with a 10^{-2}M $Ru(bpy)_3Cl_2$ solution, both at pH 3.0. Based on test results from these devices, the next films incorporated 10^{-2}M concentration of sodium tetrafluorobotate into the polymer wells for dipping. They were subsequently loaded with only the $Ru(bpy)_3Cl_2$ salt at varying pH. The next films included the same concentration of $NaBF_4$ in the polymer solutions with the addition of adding a 10^{-2}M concentration of

$NaBF_4$ to the rinse baths as well. The incorporated counterion salt was then changed from $NaBF_4$ to $TBABF_4$ to ascertain whether the cation has an effect on the device performance. $TBABF_4$ was added first only to the polymer baths and then to both the polymer and de-ionized water baths at a concentration of 10^{-2}M.

A 1200 Å thick silver electrode was evaporated on top of the films in a vacuum chamber at a pressure of 1.0-3.0 x 10^{-6} torr at a rate of 3 Å/s for the first 400 Å and 5 Å/s for the next 800 Å. The configuration of the devices on the slides is shown in Figure 2.2. The active area of each light-emitting cell was 2 mm x 3 mm.

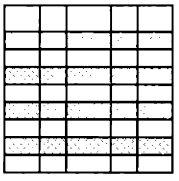

Figure 2.2: Configuration of devices fabricated on a 1" x 1" glass slide with vertical patterned strips of ITO. The horizontal stripes represent the evaporated Ag cathode and the intersection of the ITO and Ag comprises the device area.

The devices were stored and tested in a glove box filled with nitrogen. Voltage, current, and light output were measured using an HP3245A universal source, an HP34401A multi-meter and a Newport 1830-C optical power meter controlled by LabView (National Instruments). The electro-luminescence emission of all devices was red-orange, centered at around 630 nm. In the experimental setup, a calibrated photodiode was placed in front of the device at a fixed distance (10.5 mm). In this configuration, the light emitted at an angle q between 0° and 28.3° in the forward direction is collected by the photodiode.

Thickness measurements for the films were taken using a Tencor P10 profilometer in air.

2.3. Chapter 2: Results and Discussion

The first devices were made from PAA and PAAm multilayer films into which $NaBF_4$ and $Ru(bpy)_3Cl_2$ salts were sequentially loaded. The results from these devices showed extremely low luminance, 0.45 cd/m^2, at 16 volts, with a turn-on voltage of 10 volts as shown in Figure 2.3.

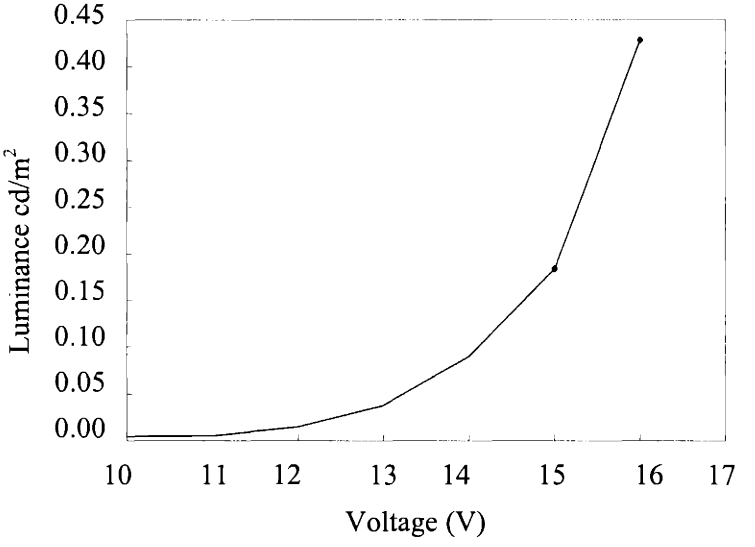

Figure 2.3: Voltage vs. luminance in cd/m^2 for a 6-bilayer LEC fabricated from a PAA (3.0)/PAAm (3.0) platform into which $NaBF_4$ and $Ru(bpy)_3Cl_2$ were sequentially loaded. These devices have low luminance at high voltages.

It immediately became a goal to reduce the turn-on voltage and increase the luminance. In order for these LEC to emit light, the BF_4^- ions must accumulate near the anode and the $Ru(bpy)_3^{2+}$ ions near the cathode to facilitate charge injection – if both types of ions are not present no emission will occur. It was hypothesized that during loading of $Ru(bpy)_3Cl_2$ into the film, the BF_4^- is released from the film back into solution. Thus a method was devised to hold the BF_4^- in the films while the Ru^{2+} was added: adding the

$NaBF_4$ salt to the polymers before dipping the substrate and forming the film. It is known that these films swell in water and saline solutions [8]. During the film formation it is likely that the film swells and the solution containing BF_4^- ions penetrates the layers. As the film is removed from solution and dried the BF_4^- could be retained in the film.

$Ru(bpy)_3Cl_2$ was loaded into 6-bilayer $NaBF_4$ films at pH 3, 6, 7, and 9. As the pH increases, so does the number of negative charges in PAA, as the COOH group becomes deprotonated. As expected, the amount of Ru^{2+} ions that was loaded into the

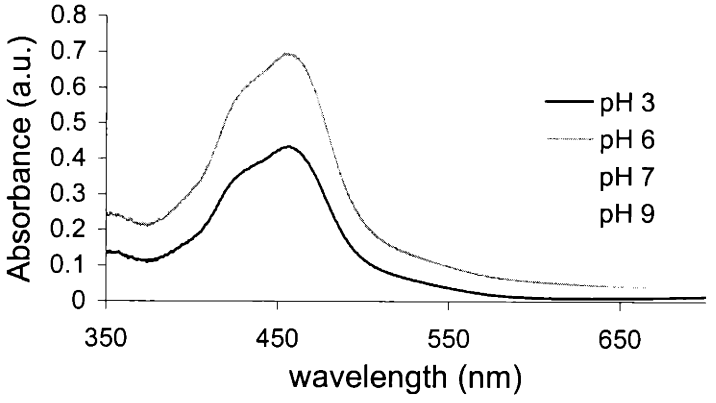

Figure 2.4: Uv-vis absorbance spectra, absorbance vs. wavelength of 6-bilayer $NaBF_4$ platform PAA (3.0)/PAAm (3.0) films loaded with $Ru(bpy)_3Cl_2$ at varying pH. As pH increases the number of ionized groups that bind to $Ru(bpy)_3^{2+}$ ions also incrases.

film increased with increasing pH. This increase can be seen in the absorbance spectra in Figure 2.4, as the Ru^{2+} ions absorb light at 450 nm and lend an orange color to the films. It can also be seen in the thickness of the film as more Ru^{2+} ion are absorbed, as shown in Figure 2.5. Loaded film thicknesses range from 498 to 652 angstroms.

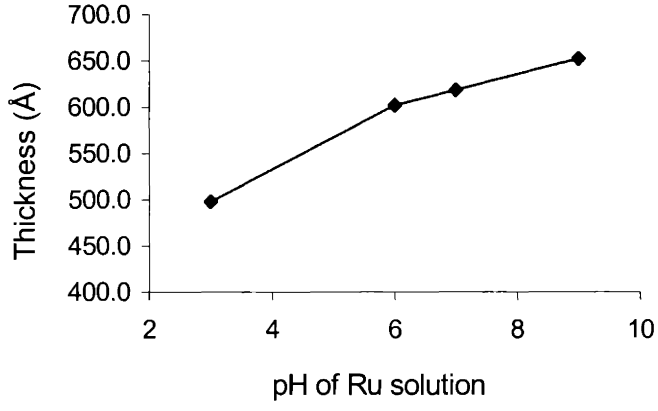

Figure 2.5: Profilometry thickness measurements of $NaBF_4$ platform PAA (3.0)/PAH (3.0) films loaded with $Ru(bpy)_3Cl_2$ vs. pH of loading solution. As pH increases, more COOH groups in PAA become ionized and more $Ru(bpy)_3^{2+}$ ions are bound, creating thicker films.

The devices fabricated from these loaded films were tested by ramping the voltage from 0-9 volts, and observing the luminance with a photodiode. The resulting voltage vs. luminance curves for the devices loaded at pH 3, 6, and 7 are shown in Figure 2.6. There was no luminance from the device loaded at pH 9.

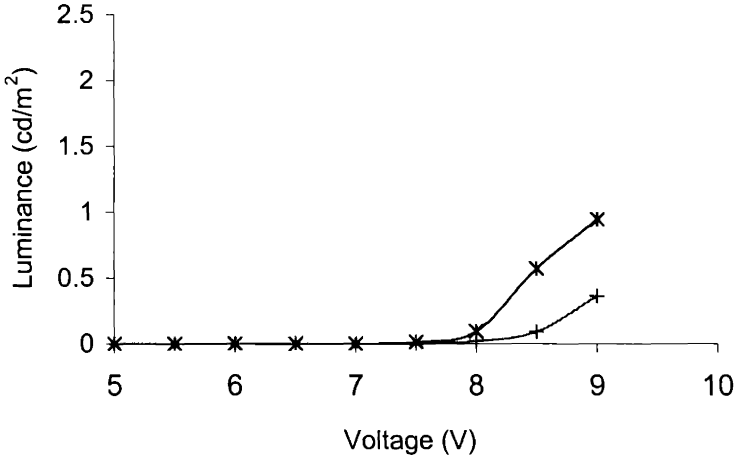

Figure 2.6: Luminance as voltage is ramped from 5-9V of devices fabricated from 6-bilayer NaBF4 platform PAA (3.0)/PAH (3.0) films loaded with $Ru(bpy)_3Cl_2$. Each curve represents a different loading solution pH. Top curve is pH 3.0, middle is 6.0, bottom is 7.0. Turn on-voltage for pH 3.0 is around 6V, for pH 6.0 around 7V, and pH 7.0 around 8V

Comparing Figure 2.6 to Figure 2.3, it has been shown that the method of binding the BF_4^- ions into the films by adding the salt to the polymer has successfully increased the luminance and reduced the turn-on voltage of the devices. From Figure 2.6, it can also be seen that pH 3 was the best loading condition for the $Ru(bpy)_3Cl_2$ salt. Most likely this is because the devices loaded at higher pH are so thick that the ions do not move quickly enough or accumulate well enough at the electrodes to facilitate charge injection.

The next logical step in this process was to add $NaBF_4$ to the rinse baths as well as to the polymer solutions to increase the concentration of counterions in the film. These devices were loaded with $Ru(bpy)_3Cl_2$ salt at pH 2 and pH 3. Devices with salt added only to the polymer solutions were fabricated as a reference and loaded in the same way. Voltage vs. luminance curves for these devices are shown in Figure 2.7.

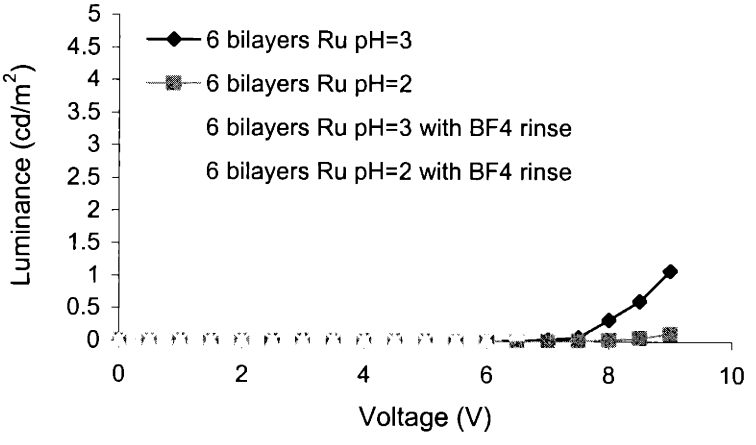

Figure 2.7: Luminance vs. voltage for loaded 6-bilayer device platforms made with $NaBF_4$ added to only the polymer dipping solutions or to both the polymer dipping solutions and the rinse baths. Devices were loaded with $Ru(bpy)_3Cl_2$ at pH 2 and pH 3. Devices with NaBF4 in the rinses consistently have higher brightness than those without, and devices loaded at pH 3 perform better than

This figure shows the improvement between the devices fabricated using the salt rinse and those without. It also shows that loading $Ru(bpy)_3Cl_2$ at pH 3 produces better quality

devices than loading $Ru(bpy)_3Cl_2$ at pH 2. This most likely occurs due to the amount of $Ru(bpy)_3^{2+}$ ions that are loaded into the film – more at pH 3 than at pH 2. The performance of these devices shows that pH 3 is the optimum pH for loading.

To investigate the effect of the type of BF_4^- salt added to the PAA/PAAm platform, films were fabricated using $TBABF_4$ added to the polymer solutions and the rinse. Films were made varying the number of (PAA/PAAm) bilayers, using pure water rinse and salt solution rinse, and loaded at varying pH. Many differences were observed between the films fabricated using $TBABF_4$ and the original $NaBF_4$ films. Results from luminance tests are shown in Figure 2.8.

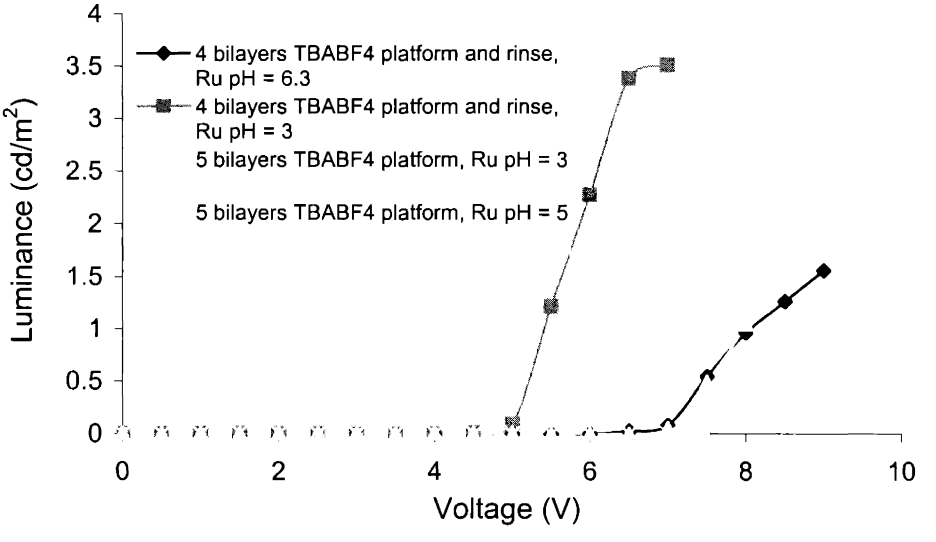

Figure 2.8: Luminance as voltage is increased in 4- and 5-bilayer devices made from adding $TBAPF_4$ to the polymer solutions or to the polymer solutions and the rinses before loading $Ru(bpy)_3Cl_2$ at various pH. The devices to which $TBABF_4$ was added to the rinse and those loaded at pH 3.0 showed higher luminance than their counterparts.

Again the devices in which the salt was added to the rinse baths showed superior performance to those fabricated with pure water rinses. The films with four bilayers have higher luminance, as well as those films loaded at pH 3. Due to the higher thickness per

bilayer than in the $NaBF_4$ platform, the $TBABF_4$ multilayer films are able to be made into devices with fewer bilayers. This allows the measured devices to be thinner, lowering the turn-on voltage, as the ions have less space to traverse. Devices fabricated from four bilayer $NaBF_4$ films showed no emission. However, the maximum luminance of $TBABF_4$ devices before they begin to fade is lower than that of the thicker devices from the $NaBF_4$ platform, showing decreased stability in operation. Figures 2.9-a and b

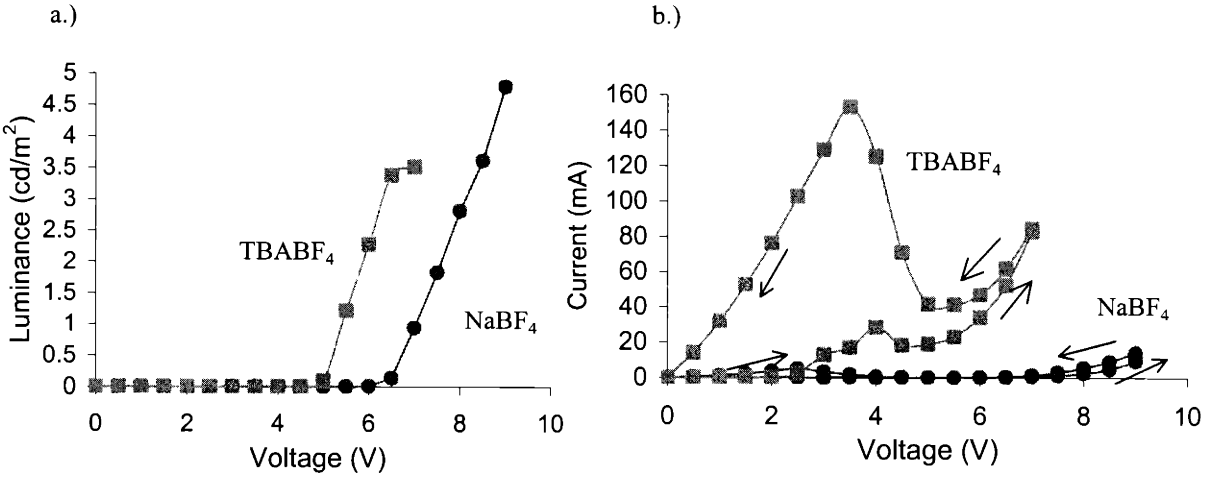

Figures 2.9a and b: Behavior of best-performing $TBABF_4$ (▪) and $NaBF_4$ (•) devices. Both devices had salt added to both the polymer solutions and to the rinse baths and were loaded at pH 3.0. The $TBABF_4$ device was 4 bilayers while the $NaBF_4$ device was 6 bilayer. 2.9a shows luminance vs. increasing voltage. The $TBABF_4$ device has a lower turn-on voltage but lower maximum emission. 2.9b shows current vs. increasing and decreasing voltage. The $TBABF_4$ device is thinner and thus has higher current. Both devices show peaks of leakage current between 2.5V and 3.5V.

compare the luminance and current for the best performing of both types of devices. As is expected, the current is higher in the thinner $TBABF_4$ films. However, the large amount of leakage current is not expected or desired, nor is the behavior of rising and dropping current as the voltage increases.

To attempt to reduce leakage current, $NaBF_4$ was added to only PAAm and to the rinses following the PAAm bath. This tests the possibility that the positive salt ions contribute to the strange current effects in the voltage ramping by producing more uneven

films that have a higher possibility of defects such as pinholes. Theoretically and experimentally the films formed with salt added to only one polymer dipping solution are thinner at a comparable number of bilayers, as less adsorbed ions causes less swelling. These data are shown in Table 2.1.

Table 2.1: Compared profilometry thickness measurements of 5, 6, and 7 bilayer devices fabricated with NaBF4 added to the PAAm dipping solution or to both the PAA and PAAm polymer solutions.

Thickness Å		
bilayers	salt in PAAm only	salt in both polymers
5	180	405
6	197	578
7	233	917

Because there was no salt added to the PAA, which contains negatively charged COO^- groups, the Na^+ ions from $NaBF_4$ should not be present and interfere with the performance of the device. Electrically, the current behavior was different. As shown in Figure 2.10 the leakage current was still present. However, instead of rising on the voltage ramp down, it rose on the voltage ramp up and was smooth on the ramp down.

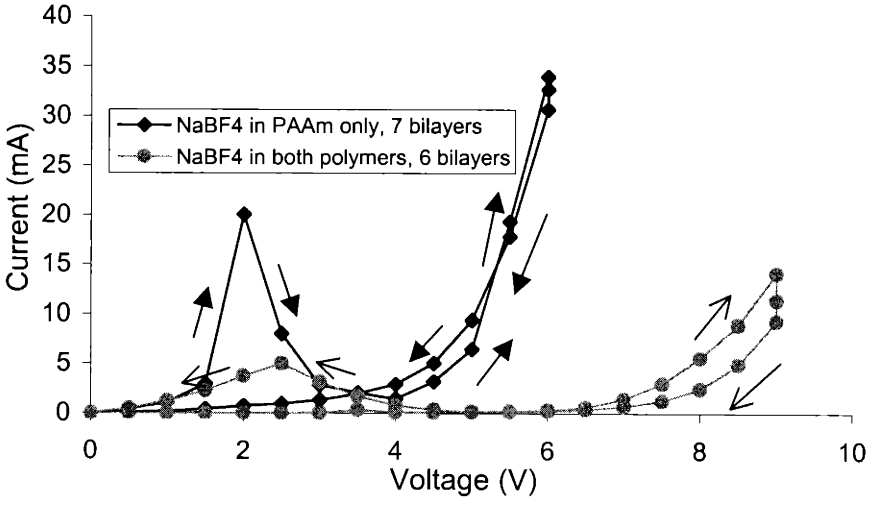

Figure 2.10: Compared current vs. voltage characteristics for devices fabricated using $NaBF_4$ in only the PAAm dipping solution and in both the PAA and the PAAm dipping solutions. Both devices showed a leakage current peak between 2 and 3V. However, in the device fabricated with $NaBF_4$ in only the PAAm the peak was on the voltage ramp up, a unique behavior in this work.

The preliminary results from all the devices fabricated are shown in Table 2.2. As a general trend, the thinner the devices, the lower the turn-on voltage, and the higher the current. Those devices in which salt was added to the rinse baths performed better in luminance testing than those without salt in the rinses.

Table 2.2: Summary of performance characteristics of $Ru(bpy)_3$ LECs fabricated from PAA (3.0)/PAAm (3.0) multilayer films.

PAA/PAAm Platform	Turn-On Voltage	Thickness / bilayers of best device	Max. Emission Observed (cd/m2)	Comments
NaBF4	6.5V	6 bilayers 602 angstroms	2.21 at 9V	Low emission, high turn-on voltage, thick film.
NaBF4 with rinse	6.0V	6 bilayers 410 angstroms	4.78 at 9V	Best emission, but turn-on voltage is still high. Low current.
TBABF4	7.0V	4 bilayers	2.67 at 9V	Low emission, high turn-on voltage.
TBABF4 with rinse	5.0V	4 bilayers 260 angstroms	3.51 at 7V	Low turn-on voltage, more stable thinner films, but very high leakage current.
NaBF4 in PAAm and PAAm rinse	4.5V	7 bilayers 233 angstroms	1.47 at 6V	Low emission, low lifetime, but low turn-on voltage and low leakage current.

2.4. Chapter 2: Conclusion

As shown in Table 2.2, this work has demonstrated that it is possible to construct LEC's by loading the cation $Ru(bpy)_3^{2+}$ into hydrogen-bonded PAA/PAAm multilayer

films. Over the course of this work device properties such as luminance and turn-on voltage have improved from 0.4 cd/m^2 at 16 volts to 4.78 cd/m^2 at 9 volts. The fabrication of these devices was done using only water-based solutions, and is possible over large areas.

Unfortunately, the device properties are still not comparable to the device properties that have been demonstrated through other fabrication techniques such as spin-coating. The turn-on voltages are still much higher while the luminances are much lower [3]. Thus, while the devices were successfully demonstrated, they are not suitable for any practical applications.

References:

[1] Slinker, Bernards, Houston, Abruna, Bernhard, and Malliaras. "Solid-state electroluminescent devices based on transition metal complexes". *Chem. Commun.* 2003: 2392-2399.

[2] Rudmann, Shimada, and Rubner. "Solid-State Light-Emitting Devices Based on the Tris-Chelated Ruthenium(II) Complex. 4. High-Efficiency Light-Emitting Devices Based on Derivatives of the Tris(2,2'-bipyridyl) Ruthenium(II) Complex". *J. Am. Chem. Soc.* 124 (17): 4918-4921

[3] Rudmann and Rubner. "Single layer light-emitting devices with high efficiency and long lifetime based on tris(2,2' bipyridal) ruthenium(II) hexafluorophosphate". *J. of Applied Physics* 90 (9): 4338-4345. 2001

[4] Wu, Yoo, Lee, and Rubner. "Solid-State Light-Emitting Devices Baesd on the Tris-Chelated Ruthenium(II) Complex: 3. High Efficiency Devices via a Layer-by-Layer Molecular-Level Blending Approach". *J. Am. Chem. Soc.* 1999, 121: 4883-4891.

[5] Chung and Rubner. "Methods of Loading and Releasing Low Molecular Weight Cationic Molecules in Weak Polyelectrolyte Multilayer Films". *Langmuir* 2002, 18: 1176-1183.

[6] Yang and Rubner. "Micropatterning of Polymer Thin Films with pH-Sensitive and Cross-linkable Hydrogen-Bonded Polyelectrolyte Multilayers". *J. Am. Chem. Soc.* 124, 10: 2100-2101. 2002.

[7] Choi, J and Rubner, M.F. Unpublished data.

[8] Yang, Mendelsohn, and Rubner. "New Class of Ultrathin, Highly Cell-Adhesion-Resistant Polyelectrolyte Multilayers with Micropatterning Capabilities". *Biomacromolecules* 2003 4: 987-994.

3. Improvements in Efficiency and Lifetime of Spin-Cast $Ru(bpy)_3$ LEC's

3.1: Chapter 3: Introduction

The experiments described in this paper aim to explore two aspects of $Ru(bpy)_3^{2+}$ LEC's that must be improved before these devices can be used in practical applications; the external efficiency and lifetime. Previous work [1] indicates that there are many ways to increase both efficiency and lifetime including modifying the bipyridyl ligands, driving the devices using AC voltage, changing the counterions, and blending the $Ru(bpy)_3^{2+}$ complexes with a polymer in spin-cast films. In 2001, Rudmann and Rubner showed that by blending films that contained PF_6^- counterions with either 25% polycarbonate (PC), 25% poly(methyl methacrylate) (PMMA), or 25% polystyrene (PS) and driving using AC voltage at 50% duty cycle, device half-lives between 500 and 1100 hours could be achieved [2]. In this work we further investigate the effects of blending the films with PMMA, PC, and PS, as well as introducing a new polymer blend in fabricating devices using 25% poly(vinylcarbazole) (PVK). The monomer unit structure of these polymers is shown in Figure 3.1. In addition, the effect of silver cathode thickness and of a stacked silver and aluminum cathode on device lifetime is studied.

Poly(vinylcarbazole) is a good candidate for a blending polymer for several reasons. It is a wide-band-gap semiconducting polymer and can function as a blue-emitting active layer in polymer light-emitting diodes [3,4]. It is capable of transporting holes and electrons, and exciton lifetimes can be several tens of nanoseconds [4]. After

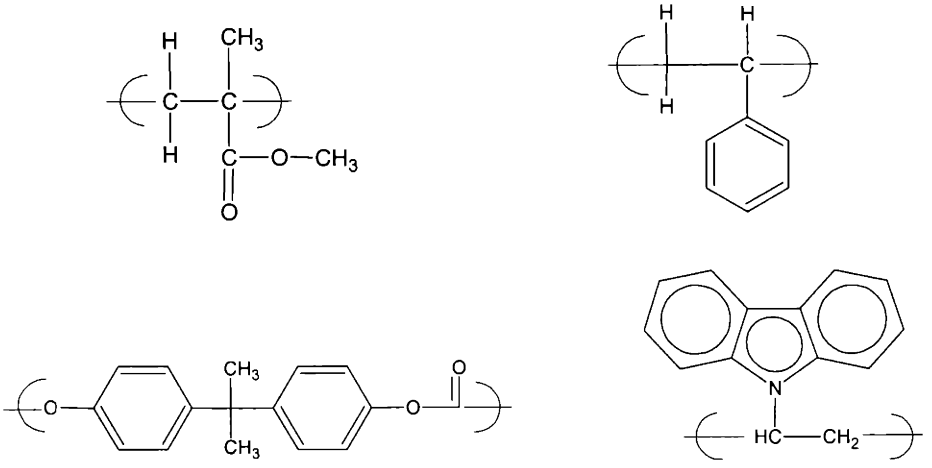

Figure 3.1: Monomer repeat units of (clockwise from upper left) poly(methyl methacrylate), polystyrene, poly(vinylcarbazole), and polycarbonate.

this work was begun, devices have also been reported that utilize an active layer of PVK doped with a small percentage of transition metal complexes such as $Ru(bpy)_3^{2+}$ complexes and $Ir(ppy)_3$ derivatives, confirming the compatibility of these materials [3]. It was observed that Förster energy transfer occurs between the host polymer and the dopant molecules in these devices [3]. Both types of PVK LEDs emit light at voltages that are much higher than the voltage required for light emission in a $Ru(bpy)_3^{2+}$-based LEC and have much lower efficiency.

Cathode thickness and structure were investigated in an attempt to improve devices lifetimes. Unlike OLEDs, $Ru(bpy)_3^{2+}$-based LECs do not require a low work-function cathode. This is because the buildup of counterions next to the cathode causes a potential drop large enough to decrease the barriers to charge injection [5]. Previous investigation showed that silver is an ideal material because it is stable in both the on and off states over long periods of time, as opposed to aluminum, which degrades the device, shortening its shelf-life [6]. In this study, the thickness of the silver cathode was varied and device half-life was measured. In addition, stacked cathode structures were fabricated

using a lower silver layer in contact with the $Ru(bpy)_3^{2+}$ film covered by either a layer of tin or aluminum. Half-life measurements for these devices were taken as well.

All devices in the current experiments utilized tetrafluoroborate (BF_4^-) counterions as opposed to hexafluorophosphate (PF_6^-) counterions because they reduce the response time of the devices and are more practical for applications. As shown by Rudmann et al. [1], devices using PF_6^- counterions have longer lifetimes than those using BF_4^-. Thus, all the measured lifetimes are expected to increase by two orders of magnitude if PF_6^- were to be used as the counterion. In addition, all data was taken using DC voltage. Thus, these measured lifetimes can also be increased using AC driving voltage. It is expected that under the previously optimized conditions, these devices would have longer lifetimes and higher efficiencies than any previously reported device.

3.2. Chapter 3: Experimental

Tris(4,4'-di-tert-butyl-2,2'-bipyridyl)ruthenium(II) ditetrafluoroborate complex [t-bu Ru(bpy)3](BF4)2 was prepared from [t-bu $Ru(bpy)_3]Cl_2$ complex through ion exchange with an excess of $NaBF_4$ in deionized water. The [t-bu $Ru(bpy)_3](BF_4)_2$ was recrystallized twice by dissolution in acetone followed by precipitation in deionized water. The resulting material was dried under vacuum overnight at 80C and stored under nitrogen.

Patterned ITO glass substrates were cleaned as described in the previous chapter. Prior to spin coating, the glass slides were plasma cleaned for 5 minutes in a Harricks plasma cleaner in air.

All films were prepared by spin coating at 1500 rpm for 30 seconds under a nitrogen atmosphere. The solutions were filtered using a 0.2-micron membrane filter before spin coating. Various solvents were used with the varying polymers. Acetonitrile was used with no polymer, PMMA, and PC blends, toluene was used with PS blends, and dichloromethane was used with PVK blends. The concentration of the acetonitrile, toluene, and dicholormethane solutions was adjusted to give the desired final film thickness for devices when spun at 1500 rpm.

The spun films were dried under vacuum for 2 hours at 120°C. They were then cooled over night in the vacuum oven.

Cathodes were evaporated as described in the previous chapter. The configuration of devices is shown in Figure 2.2.

The active area of each light-emitting cell again was 2 mm x 3 mm, and the emission was again red-orange, centered around 630 nm. The devices were stored and tested in a glove box under a nitrogen atmosphere. All devices were tested under a DC voltage using the same setup and equipment as described in the previous chapter.

Thickness measurements for these films were taken using both profilometry and ellipsometry techniques.

3.3. Chapter 3: Results and Discussion

Photoluminescence measurements were taken of films of increasing thickness for each polymer-blended film: PMMA, PC, PS, and PVK. During LEC operation, due to the counterion buildup at the cathode the junction between the cathode and active layer is ohmic, which ensures that every injected electron combines with a hole to form an exciton. This means that the device efficiency is determined by the photoluminescence of the active layer [5]. As shown in Figure 3.2, PVK blends show not only a higher photoluminescence than the other polymers, but also a steeper slope as the thickness and light absorbance of the film increases. This leads to the expectation of increased

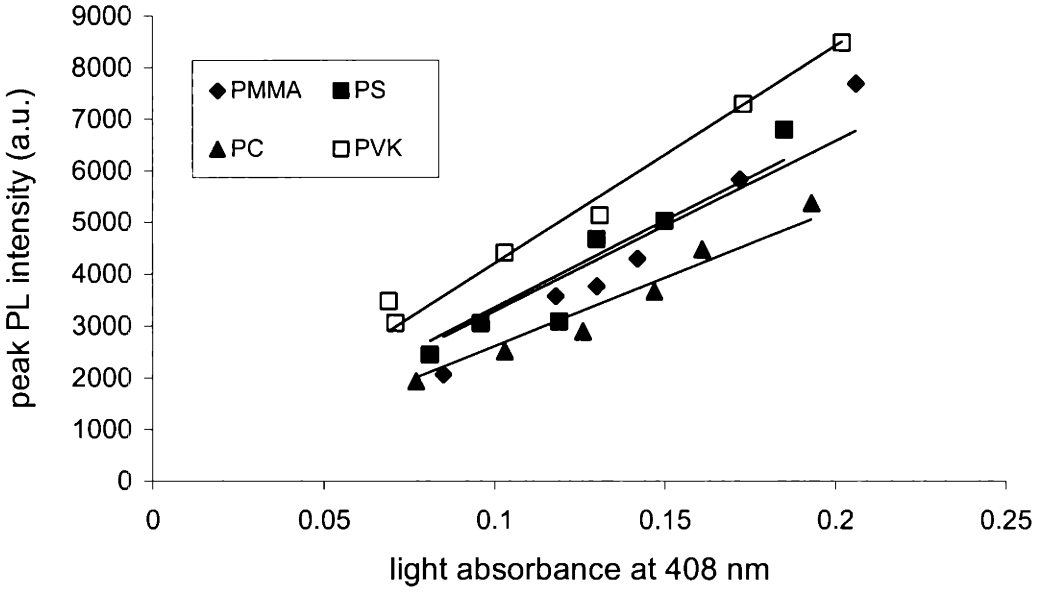

Figure 3.2: Peak photoluminescence for films of increasing light absorbance and film thickness for films of $Ru(bpy)_3$ blended with PMMA, PS, PC, and PVK. Linear fits are shown. PVK has highest photoluminescence for all light absorbencies.

electroluminescence in PVK blends. It is known that the act of dispersing the $Ru(bpy)_3^{2+}$ complex into a polymer matrix increases the intensity of the PL spectrum [1]. However,

too much polymer added decreases the film conductivity, which decreases the electroluminescent efficiency by requiring a higher driving voltage. The polymer blends used were all 25% polymer, which still allows the ions enough mobility to operate the devices at low voltage. Figure 3.3 shows the initial ramping voltage test performed on each sample. The voltage is increased by 0.1V increments, holding for 5 seconds at each voltage. Turn-on voltage for all samples falls between 2.2-2.4V. The $Ru(bpy)_3[BF_4]_2$ films with no added polymer show the greatest luminance. However, these films are not stable, as the lifetimes of these devices are extremely short, on the order of minutes.

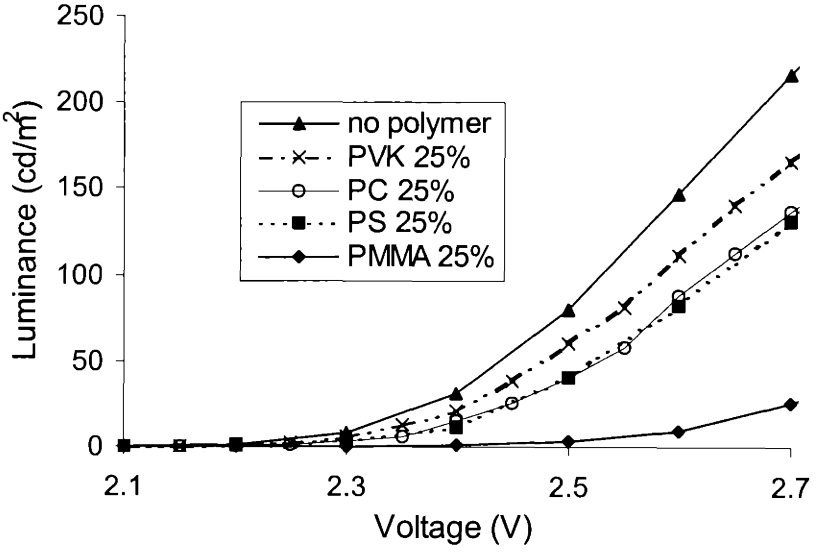

Figure 3.3: Luminance vs. voltage for spin-cast films of $Ru(bpy)_3$. The highest luminance (but most unstable film) is that without a polymer blend. Data for films of polymer blends of 25% PVK, PC, PS, and PMMA are shown. PVK shows the highest luminance of any polymer blend.

Pure $Ru(bpy)_3[BF_4]_2$ film devices have low resistance. This higher current through the devices leads to faster breakdown due to coulombic oxidation and reduction. Thus for the devices to be able to be used in practical applications the films must be stabilized using polymer blends. A polymer allows the films to emit light while decreasing the current

through the film that leads to breakdown. This allows for a device with increased efficiency. Each of these polymer blends allows for a different degree of emission. The PVK has the highest emission, followed by the PC, then the PS, and finally PMMA. The next step is to find the efficiency of these devices.

The thickness of the films was varied by varying the ratio of solvent to polymer and $Ru(bpy)_3[BF_4]_2$ in the precursor solution. Each device was held at 2.5V until a plateau luminance had been reached and the luminance began decaying. The peak efficiency at the plateau luminance was taken as the measured efficiency for the device. Figure 3.4 shows the film thickness vs. efficiency plot for the polymer blend devices. All polymer devices show a parabolic dependence of efficiency on thickness, with a maximum at around 150 nm. The devices blended with PVK had the highest efficiencies for every thickness of film measured, while the devices blended with PC had the lowest efficiencies for every thickness.

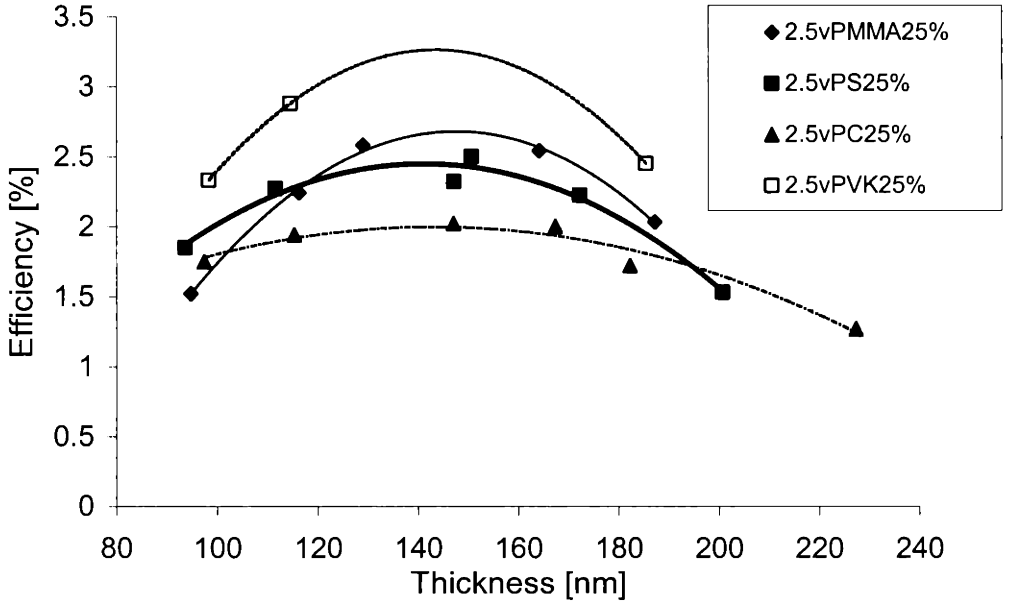

Figure 3.4: Efficiency vs. thickness for polymer blended $Ru(bpy)_3$ films. All films show a parabolic dependence. PVK blends show the highest efficiency for each film thickness.

The short-timescale behavior of the devices was studied to determine response time, current flow, and efficiency. Figures 3.5a-c show luminance, current, and efficiency vs. time behavior for devices with various polymer matrices at 2.5V DC. Figure 3.5-a shows that polycarbonate devices have the highest luminance and the shortest response time, followed by PMMA. Devices from PVK are the slowest to respond but end up having a luminance comparable to PMMA, slightly higher than that of PS. In addition to having the highest luminance, polycarbonate devices have the highest current, which makes for the lowest efficiency. It is believed that because polycarbonate is somewhat hydrophilic, the slight amount of water in the device increases both luminance and current by increasing counterion mobility [5]. PMMA also has a high current, which could also be attributed to traces of water. Neither polystyrene nor poly (vinyl carbazole) contains any hydrophilic groups, and thus their current values are lower.

a.)

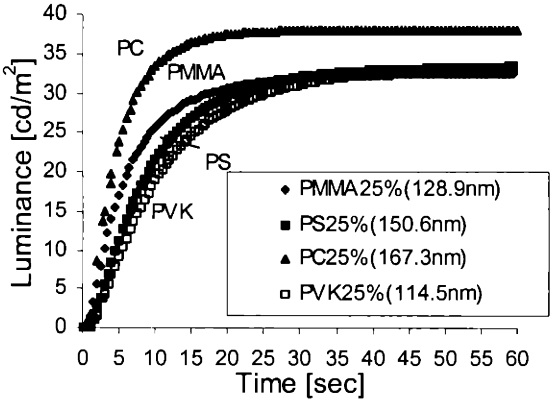

b.)

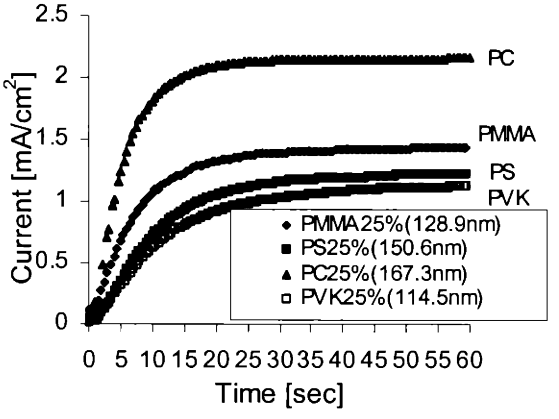

c.)

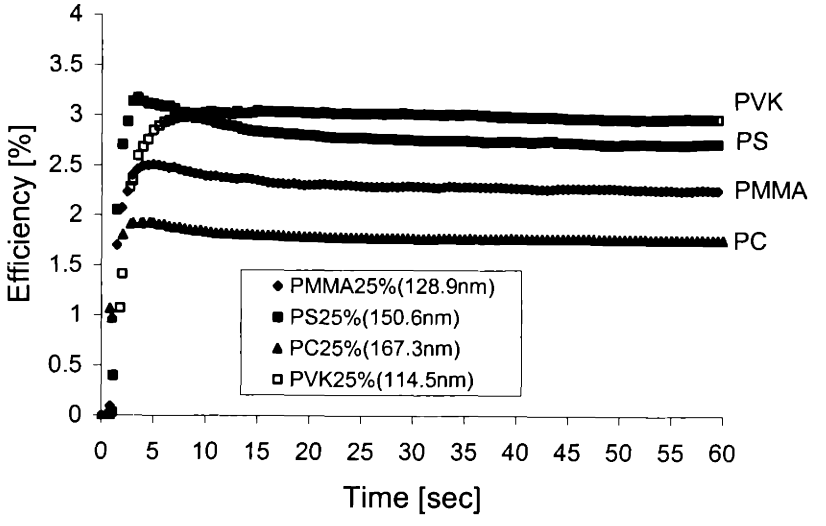

Figures 3.5a-c: Short time-scale properties of 25% polymer blends of PVK, PS, PMMA, and PC. 3.5a shows luminance response time at 2.5 applied volts, 3.5b shows current response time at 3.5 applied volts, and 3.5c shows efficiency at short timescales at 2.5 applied volts.

The devices from PVK show the highest plateau efficiencies, at just over 3%. PS devices show higher initial efficiency, but this quickly decays, as the luminance response time is faster than the current in these devices.

At longer timescales the aim is to attain the highest quality devices for the longest amount of continual operation time. 2.5V DC were applied to the devices which were allowed to run until the half-life was able to be calculated. The half-life is defined as the time at which the luminance has decayed to half its original value.

Figure 3.6 shows the efficiency of these devices over long timescales. The efficiency decays at a different rate for each polymer. The devices made from PC and PMMA decay fastest, most likely due to the traces of water facilitating the formation of quenching species near the cathode in the films [7]. The devices fabricated with PVK begin at a higher efficiency, and maintain that higher efficiency for the longest amount of time.

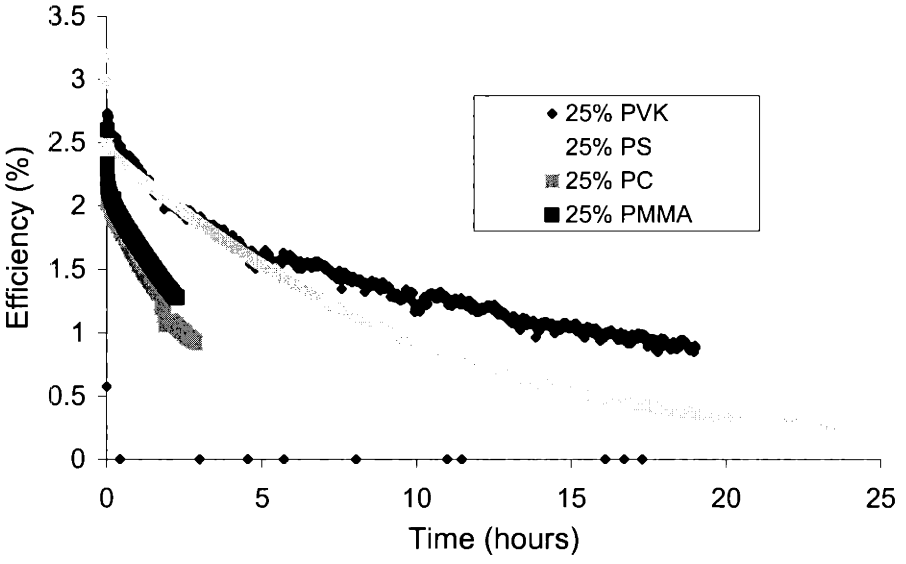

Figure 3.6: Long timescale vs. efficiency measurements for each polymer blend. Lowest initial efficiency and fastest decay occurs in PC blended films. Highest initial efficiency and slowest decay occurs in PVK blended films.

Another factor that has an effect on the long-term performance of these devices is the cathode, its materials and structure. Unlike other OLEDs these devices do not require low work-function metals [5]. For the devices examined in these experiments silver cathodes were used. In addition, devices with stacked cathodes were fabricated: tin on silver and aluminum on silver. Figure 3.7 shows the results of lifetime testing on these devices. Varying the thickness of the silver-only cathode had a minimal effect on the device half-life. However, the use of stacked cathodes increased the lifetime, most particularly Å stacking aluminum on top of silver, at all initial luminances. This could be because aluminum acts as a heat sink for the device, preventing the formation of quenching

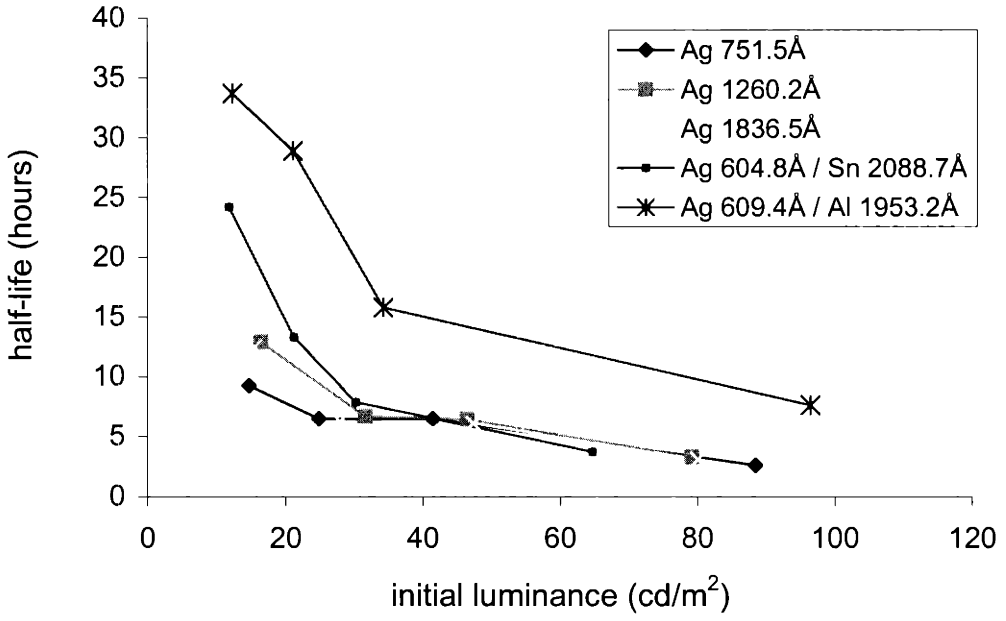

Figure 3.7: Half-life dependence upon initial luminance for various cathode structures in 25% polystyrene blended devices. In all cases half-life increases with lower initial luminance.

species through thermal energy. Also, because water enhances quenching species formation, the enhanced lifetimes could also occur because the capping layer acts as an additional barrier to moisture entering the active layer.

A summary of the findings from various tests on the devices fabricated with each polymer is found in Table 3.1. At each polymer device's peak efficiency, the PVK device has the highest efficiency, the PS device the longest lifetime, and PC the highest luminance (although they all are comparable) and the fastest response time. These devices, to be used in practical applications, would ideally have a fast response time, high efficiency, and long half-life. Based on these data, no one polymer blend satisfies all of these criteria, although PS and PVK are close.

Table 3.1: Summary of $Ru(bpy)_3$ LEC's with blended polymer films. Based on properties and data, two categories of polymer blends emerge: PC and PMMA and PS and PVK.

Polymer 25% at 2.5V						
	Response Time [s]: t (to 5cd/m^2)	Response Time [s]: t (to plateau)	Luminance [cd/m^2]	External Efficiency [%]	Thickness [nm]	Half life [hours]
PC	1.5	32.5	37.8	1.75	167.3	2.5
PMMA	1.9	40.9	32.3	2.25	128.9	1.9
PS	3.0	53.0	33.2	2.71	150.6	7.6
PVK	3.5	57.5	33.3	2.96	114.5	5.7

The polymers shown here can be divided into two categories. Polycarbonate and PMMA both yield fast response times but low efficiencies and short half-lives. They both have hydrophilic groups and are not capable of carrying charge and playing an active role in electroluminescence. Polystyrene and PVK devices have longer response times but higher efficiencies and much longer half-lives. They are both hydrophobic, and due to their aromatic side-groups could possibly assist charge transport within the active layer.

3.4. Chapter 3: Conclusion

Light emitting electrochemical cells based on the $Ru(bpy)_3$ complex were fabricated by blending the complex with 25% of various polymers: polycarbonate, poly(methyl methacrylate), polysytrene, and poly(vinylcarbazole). The operational properties of these devices were measured to obtain values for the devices' efficiencies, luminances, response times, and half-lives. Devices were also fabricated that utilized Ag cathodes of varying thicknesses and stacked cathode structures. The goals of this work

were to improve the lifetime and efficiency of the LECs so that they could be used in practical applications such as monochromatic alphanumeric displays or backlights.

The results show that the polymer blends can be placed into two categories: those that yield shorter response times (1.5-1.9 seconds), lower efficiency (1.75-2.25%) and shorter lifetimes (1.9-2.5 hours), and those with longer response times (3-3.5 seconds) but higher efficiency (2.71-2.96%) and longer lifetimes (5.7-7.6 hours). All measurements were taken at 2.5V DC. The polymers in the first category, PC and PMMA, both contain hydrophilic groups and do not contain aromatic side groups. The polymers in the second category, PS and PVK, are hydrophobic and contain aromatic side groups that could assist in charge transport in the device active layer. Thus, the goals of increasing the efficiency and lifetime of these devices has been achieved through blending the films with active, hydrophobic polymers such as PS and PVK. However these increases are paid for through a more lengthy response.

References:

[1] Rudmann, Shimada, and Rubner. "Solid-State Light-Emitting Devices Based on the Tris-Chelated Ruthenium(II) Complex. 4. High-Efficiency Light-Emitting Devices Based on Derivatives of the Tris(2,2'-bipyridal) Ruthenium(II) Complex". *J. Am. Chem. Soc.* 124 (17): 4918-4921

[2] Rudmann and Rubner. "Single layer light-emitting devices with high efficiency and long lifetime based on tris(2,2' bipyridal) ruthenium(II) hexafluorophosphate". *J. of Applied Physics* 90 (9): 4338-4345. 2001

[3] Shen, Xia, Zhang, Lin, He, and Ma. "Electroluminescence of Poly(vinylcarbazole) Doubly Doped with Two Phosphorescence Dyes: Investigation of a Spectral Change as a Function of Driving Voltage". *J. Phys. Chem. B.* 2004 108: 1014-1019.

[4] Xia, Zhang, Liu, Qiu, Lu, Shen, Zhang, and Ma. "Ruthenium(II) Complex as a Phosphorescent Dopant for Highly Efficient Red Polymers Light-Emitting Diodes". *J. Phys. Chem. B.* 2004 108: 3185-3190.

[5] Slinker, Bernards, Houston, Abruna, Bernhard, and Malliaras. "Solid-state electroluminescent devices based on transition metal complexes". *Chem. Commun.* 2003: 2392-2399.

[6] Rudmann H, Shimada S, Rubner MF, Oblas DW, Whitten JE. "Prevention of the cathode induced electrochemical degradation of [Ru(bpy)(3)](PF6)(2) light emitting devices" J. Applied Phsyics 92 (3): 1576-1581. 2001

[7] Kalyuzhny, Buda, McNeill, Barbara, and Bard. "Stability of Thin-Film Solid-State Electroluminescent Devices based on Tris(2,2'-bipyridine)ruthenium(II) Complexes." J. Am. Chem. Soc. 2003, 125: 6272-6283

4. Patterning of Polyelectrolyte Multilayer Films using Salt Solutions

4.1. Chapter 4: Introduction

Polymer blended $Ru(bpy)_3^{2+}$ LECs, due to their low turn-on voltage and high brightness, are good candidate materials for applications such as monochromatic alphanumeric displays and backlights for devices such as watches, as shown in Figure 4.1 [1].

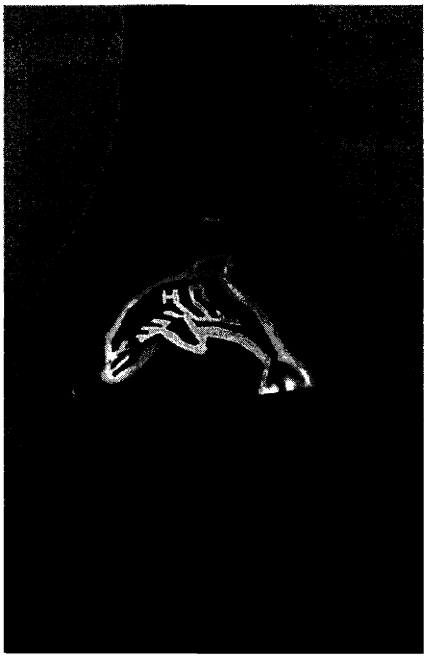

Figure 4.1: Patterned $Ru(bpy)_3$ LEC fabricated by the Rubner group at MIT for backlight applications [1].

[1]

In these applications, it would be useful to have a technique that can accurately pattern the active layer that is low cost and not potentially harmful to other sensitive materials in the manufacturing process. A promising method of handling this is to use polyelectrolyte multilayer films. These films can be fabricated onto the transparent anode and then be

subtractively patterned such that charge injection does not occur into the portion of the active layer that lies on top of the insulating film. This creates a patterned light-emitting device. The experiments reported in this chapter investigate a method of selectively etching polyelectrolyte films of poly(acrylic acid) (PAA) and poly(allylamine hydrochloride) (PAH) and controlling their thickness on the nanoscale.

Polyelectrolyte multilayer films are fabricated by adsorbing alternating layers of oppositely charged polyelectrolytes onto a substrate. The properties of the films can vary greatly depending on variables that can be controlled during their formation, such as the pH or the ionic strength of the polymer dipping solutions [2,3]. Various polyelectrolyte multilayer films have been investigated as possible candidates for materials used in drug delivery, optical communications, and patterning templates for building arrays of other materials, among other applications. Previously reported patterning techniques include polymer stamping [4], and etching the film using a strong acid [5].

In this study, etching was executed using aqueous solutions of NaCl or $MgCl_2$ at various molarities. The study primarily investigates the system of PAA deposited at pH 3.5 and PAH deposited at pH 7.5, although other systems were used to test whether the etching process can be generalized to cover all ionically bonded polyelectrolyte multilayer films. This system was chosen primarily due to its usefulness in anti-reflection coatings [5]. The bilayers in these films are very thick with lots of loops and tails in the polymer layrs [2]. It has been reported that these films can be etched completely away using a strong acid [5]. In this paper we report etching of these films using salt solutions at neutral pH, for which the film thickness can be controlled on the nanoscale. The controllable final film thicknesses as well as the use of a neutral pH are attractive

qualities of this method. As with the acid, the salt solutions can be used in conjunction with an inkjet printer to control the pattern. However, unlike acid, salt solutions are safe for longer-term use with the printing equipment as well as for any other components of the processing system.

PAA (pH 3.5)/PAH (pH 7.5) films were etched in salt solutions and then analyzed. The goal was to characterize and calibrate the etching process, and to then investigate the mechanism behind it. Based on these investigations, possible new applications were explored.

4.2. Chapter 4: Experimental

Films were fabricated using the same equipment and materials as in chapter 2. However, these films were fabricated of alternating layers of poly(acrylic acid) (PAA) (MW = 90,000 in a 25% aqueous solution) and poly(allylamine hydrochloride) (PAH) (MW = 70,000) at 10 mM concentrations based on the monomer. The PAA was at pH 3.5, while the PAH was at pH 7.5. The first layer of each film was PAH, followed by varying numbers of layer for each individual experiment. The slides were dipped into each polymer for 15 minutes, followed by three de-ionized water rinse baths for two minutes, one minute, and one minute before the next layer is added. In these films, no salts were added to either the polymers or the rinses during the film fabrication.

These films were fabricated onto single crystal silicon wafer substrates as opposed to glass in order to detect changes in the light reflected from the films.

Substrates were cut into pieces. Pieces were soaked in NaCl salt solutions of 0.5M, 1M, 2M, 3M, 4M, and 5M or $MgCl_2$ salt solutions of 0.5M, 1M, 1.5M, 2M, and 3M for one minute. They were then rinsed in three consecutive de-ionized water rinse baths for two minutes, one minute, and 30 seconds. All films were dried using compressed nitrogen. Thickness measurements were taken using profilometry or ellipsometry at an incident angle of 70° of all the etched films plus reference samples of the unetched film. Refractive index measurements were taken via ellipsometry in conjunction with the thickness measurements.

Measurements of fluorescence were taken using a microscope equipped with a green light. All pictures were taken under the same luminance conditions on previously unexposed areas of etched film. The intensity values for each molarity were found through processing the pictures in Adobe Photoshop. The values are the average of three measured values from two samples each (6 values total) of a reference film, 0.5M, 1M, 2M, 3M, 4M and 5M etched films.

4.3. Chapter 4: Results and Discussion

The first films used were 21 layers, 41 layers, and 49 layers with PAH on top. Thickness results for etching by NaCl are shown in Figures 4.2a and b. Figure 4.2a shows the actual thicknesses, while Figure 4.2b shows the relative thicknesses. As the molarity of the salt solution increases above 3, the film thickness begins to decrease. Because the films are ionically bonded, salt can affect the thickness of the film by affecting the

strength of these bonds through shielding interactions. These figures show that the overall thicknesses of these ionically bonded films are decreasing at the same relative rate at salt concentrations higher than 3M. However, whether the films are releasing material or whether they are rearranging and shrinking cannot be determined from these data.

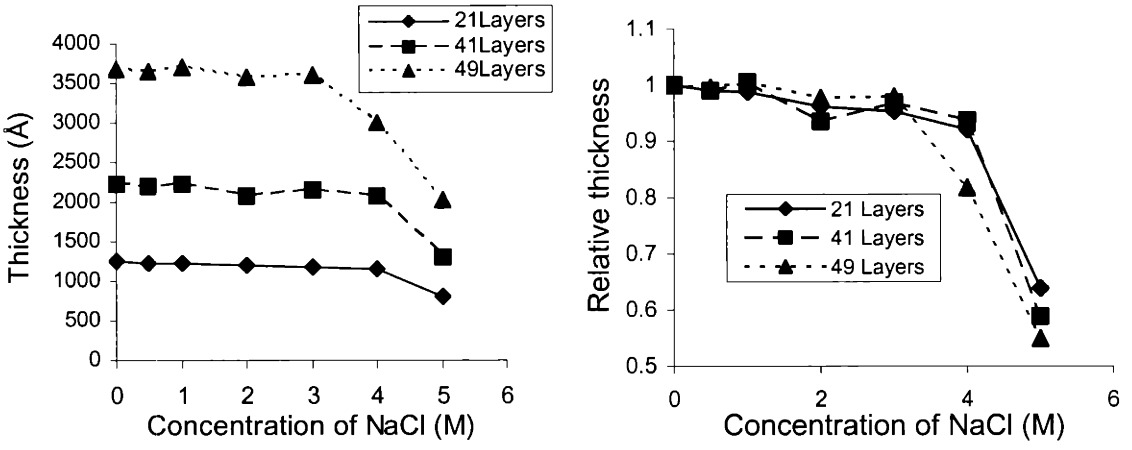

Figures 4.2a and b: Thickness measurements of PAH (7.5)/PAA (3.5) films etched using 0.5, 1, 2, 3, 4, and 5M NaCl aqueous solutions. 4.2a shows actual thickness of etched films composed of 21 layers, 41 layers, and 49 layer, while 4.2b shows relative thicknesses, demonstrating that the etching trend is the same regardless of initial film thickness. All films had PAH top layers.

logical to hypothesize that layers are being removed by the salt etching process. These films form by consecutive layers adsorbing onto the previous one through ionic bonds, the concentration of which are determined by the pH of the solution. For example, in PAA, at high pH most of the carboxyl groups are deprotonated, leaving most units with a negative charge. The molecule in solution is 50% protonated at pH 6.5 [6]. At low pH, most of the carboxyl groups are re-protonated, creating a more neutral molecule that as a consequence cannot effectively bind ionically [2]. It is known that ionically bonded polyelectrolyte multilayer films can be etched based on this principle using acid [5]. Salt has a similar effect in multilayer formation. At high ionic strength the salt reduces the strength of the ionic interactions between the polyelectrolytes, creating thicker films up to

a threshold of not binding at all [3]. By coming in and binding to the charges in the polyelectrolytes, the salt ions increase the solubility of the layers of the film. This theory is in agreement with the proposed dissolution mechanism of polyeletrolye multilayer films previously published by Dubas et. al [3].

To determine whether the observed process is dependent on the upper surface of the film, the etching was tested on films in which the top layer is PAA. Figure 4.3 shows that etching occurs in both types of films beginning at a concentration of 3M.

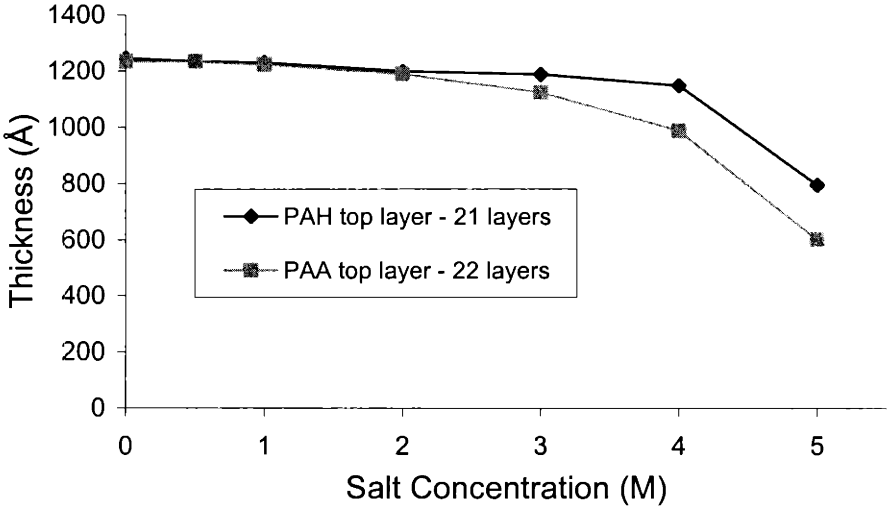

Figure 4.3: Comparison of film thickness vs. NaCl etching solution molarity for 21 and 22 layer PAH (3.5)/PAA (7.5) films with PAH as the top layer and PAA as the top layer.

The film with PAA on top decreased more than the film with PAH on top, which could be due to the difference in concentration from pH of free ionic charges on the surface of the film that can bind with the ions in the solution. It has been found that in films built from PAA adsorbed at low pH and PAH adsorbed at higher pH the PAA demonstrates a lower effective pK_a than in solution [2]. Thus a salt bath at pH 5.5 would more drastically increase the amount of charge on a PAA top layer. These surface charges interact to

change the strength of the charges in the inner layers of the film. This experiment shows that the etching phenomenon occurs regardless of the top layer of the film. However, the extent to which it occurs is different and thus for control and comparison purposes, the rest of the films used in these experiments had PAH top layers. If technique were to be used on a larger scale, separate etching calibration curves would be needed for PAA and PAH top layer films.

The next question was whether this process is specific to this system of polymers. Figure 4.4 shows a comparison of etching results from the PAA/PAH film to a film fabricated from sulfonted polystyrene (SPS) and PAH, etched using NaCl.

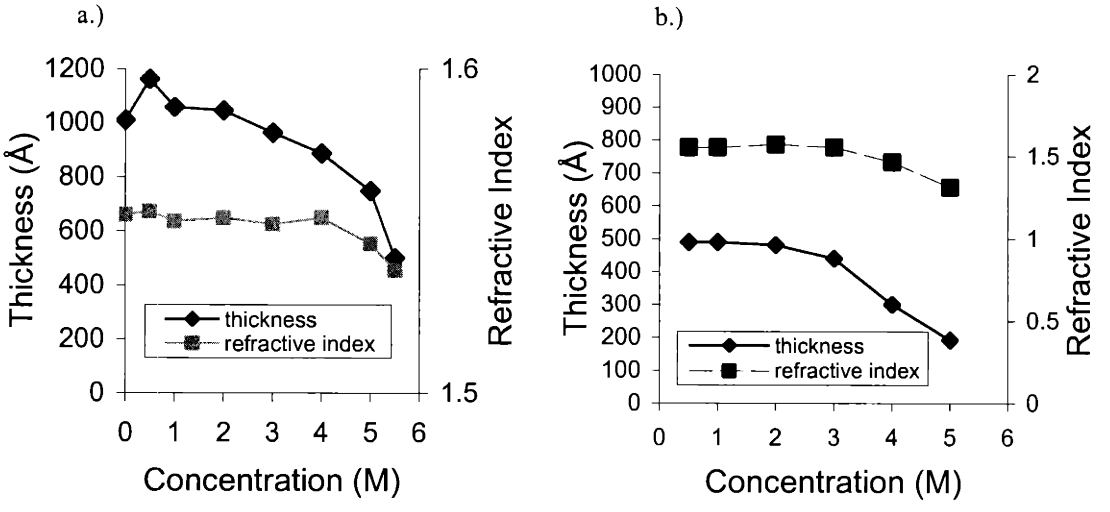

Figures 4.4a and b: 4.4a shows thickness and refractive index vs. NaCl concentration in the etching solution for PAA (3.5)/PAH (7.5) films, while 4.4-b shows thickness and refractive index vs. NaCl concentration in the etching solution for SPS (7.5)/PAH (7.5) films.

The results show that the salt etching occurs in both the ionically bonded film structures of PAA(3.5)/PAH(7.5) and SPS(7.5)/PAH(7.5) (fabricated by Koji Itano, Rubner lab, MIT). Both polyelectrolyte films show a decrease in thickness as the NaCl concentration in the etching solution gets higher than 3M. In addition, the change in refractive index

also occurs in both film types as they get thinner. In the case of SPS/PAH the change is quite significant, and may point to film microstructure rearrangement and the introduction of pores into the film. This example shows that this etching method is not limited to the PAA/PAH system, and is sensitive on the nanometer scale in other systems of polyelectrolyte multilayer films that are ionically bonded.

As shown in Figure 4.5, the thickness of PAA/PAH etched films varied depending on the salt used. A divalent salt, in this case $MgCl_2$, etches more strongly than a monovalent salt. Data shown in this graph are of films etched with solutions of 0.5M, 1M, 2M, 3M, 4M, and 5M for NaCl, and 0.5M, 1M, 1.5M, 2M, and 3M for $MgCl_2$. At a concentration of 3M of $MgCl_2$ (an ionic strength of 9) in the etching solution, the film is completely dissolved.

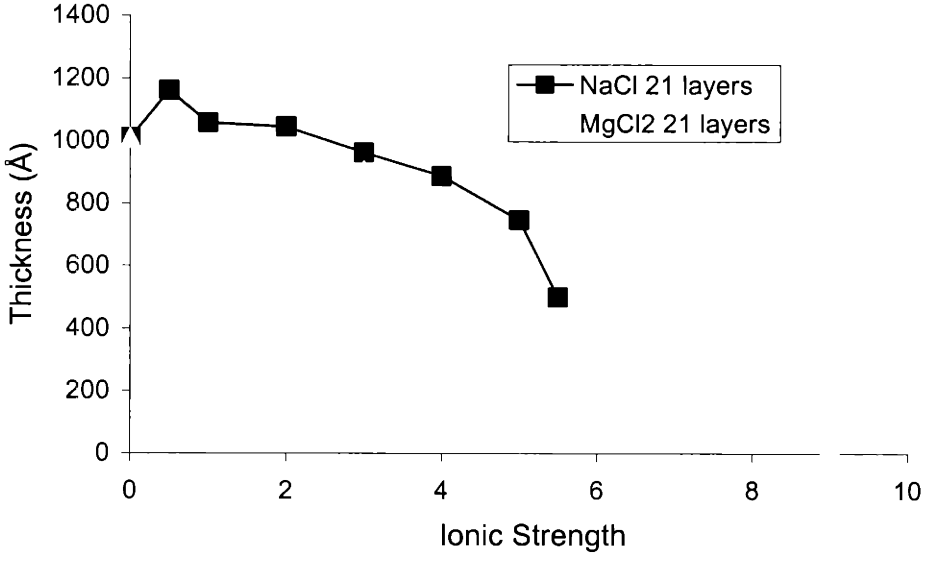

Figure 4.5: Thickness vs. ionic strength of etching solution for films etched by solutions of NaCl (■) and $MgCl_2$ ( ). In a 3M (9 units of ionic strength) solution $MgCl_2$ the film completely dissolves.

This shows that concentration not only affects the etching process, ionic strength is also a factor. The formula for ionic strength is given as follows:

$$I = \frac{1}{2}\sum_i m_i z_i^2$$

where m is the concentration of a species and z is the charge of that species. At equal concentrations [m] of $MgCl_2$ and NaCl, $MgCl_2$ has three times the ionic strength of NaCl. This is in agreement with the theory that the salt is screening charges and increasing the solubility of the multilayer films.

To further explore the potential explanation that material is being released from the films upon etching, PAH was prepared that contained the fluorescent dye fluorescein with an N-hydroxy succinimide (NHS) group that bonded to the PAH. This new form of PAH was incorporated into a 21 layer multilayer film as shown in Figure 4.6a. These fluorescent dyes emit green light upon illumination. NaCl etched samples were observed under a microscope equipped with an illumination source. The plot of fluorescent intensities from the analyzed photos of these samples is shown in Figure 4.6b. The plot shows a decrease in luminosity as the salt concentration increases, which means that the amount of material giving off a fluorescent response decreases as the film gets thinner. As the films are etched to a final height of approximately 0.6 of their initial height, some material must be lost, including the top two layers of tagged PAH, causing the detected luminosity to decrease.

Because these films were made on reflective substrates, changes in film thickness on the nanometer scale could be observed through changes in the color of the light that is reflected from the film's surface. When a film's thickness is on the order of a few wavelengths of light, changing its thickness changes the wavelengths that interfere constructively and are reflected. Using NaCl, due to a finer level of controlled etching, it is possible to fabricate films of more varying colors.

a.)

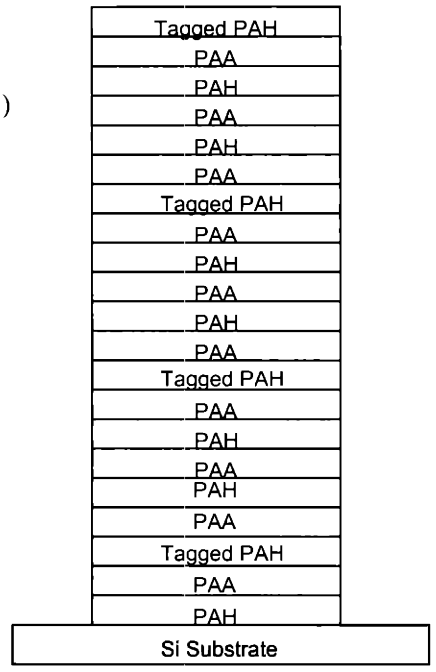

b.)

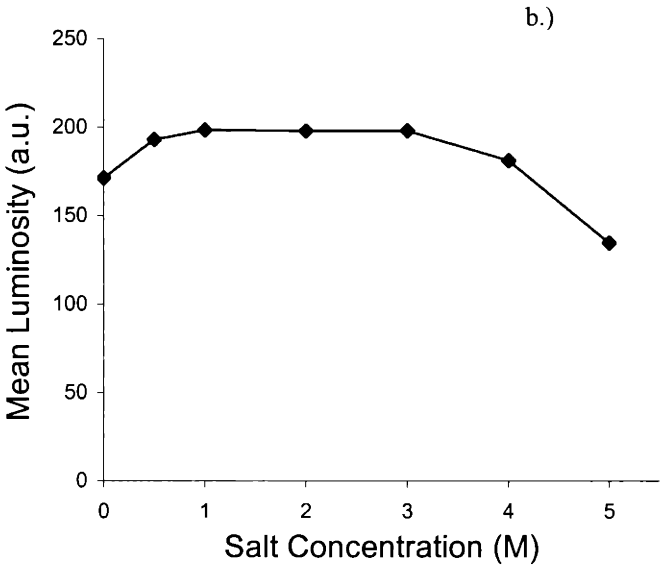

Figures 4.6a and b: 4.6a shows the layer construction of 21 layer PAA/PAH/tagged PAH films fabricated on silicon substrates to detect fluorescence luminance. Figure 4.6b shows the luminosity vs. the concentration of NaCl in the etching solution of these films.

An interesting aspect of this process is the fact that after etching a sample with a highly concentrated salt solution, immersing it into a salt solution of lower molarity has no effect either on the film's reflected color or thickness. This means that some type of rearrangement within the film and its bonds must occur. If layers were simply coming off without affecting the rest of the film, further etching would be possible at lower salt concentrations because the salt would continue to shield charges and increase film solubility. Thus it appears that the observed decrease in thickness is a combination of film rearrangement brought about by the salt and removal of the top layers of the multilayer films.

Pristine and etched films were imaged using an AFM in order to detect changes in topography and roughness to observe and characterize film rearrangement after etching. Images were taken of films composed of 21 and 49 layers of PAA and PAH etched at

various molarities of NaCl. From these images (not shown) it was clear that film surface rearrangement was occurring, but the data was inconclusive as to its nature. For the 21-layer film the lengthscale of the roughness elements increased while for the 49-layer film the lengthscale of the roughness elements decreased. Thus no clear pattern was observed even though film microstructure was confirmed to be changing.

The phenomenon of non-accumulating etching when the substrate is dipped into a bath of lower molarity than the previous etch can be exploited in patterning applications. Figure 4.7 shows a substrate that was patterned using masks. It was dipped first into 5M NaCl solution to create the yellow background. Next the 1 sticker was removed and etched in 4M solution, followed by the 2 sticker and etching in 3M solution, then the 3 sticker was removed.

Figure 4.7: Silicon substrate with 41 layer PAA/PAH film etched sequentially using NaCl at 5M, 4M, and 3M.

This effect illustrates the usefulness of this phenomenon arising from the combination of film removal and rearrangement in controlled nanoscale etching using NaCl.

One other interesting and potentially useful application of this technique is in creating a film that gradually decreases in thickness. To do this, a solution is made in which the salt concentration gradually increases from 0 to 5M from top to bottom and the substrate is immersed into this bath. Figure 4.8 shows the gradient film along with the measured thicknesses along the film's axis.

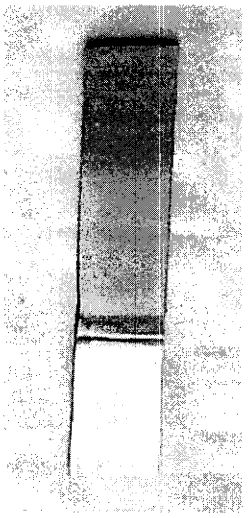

a.)

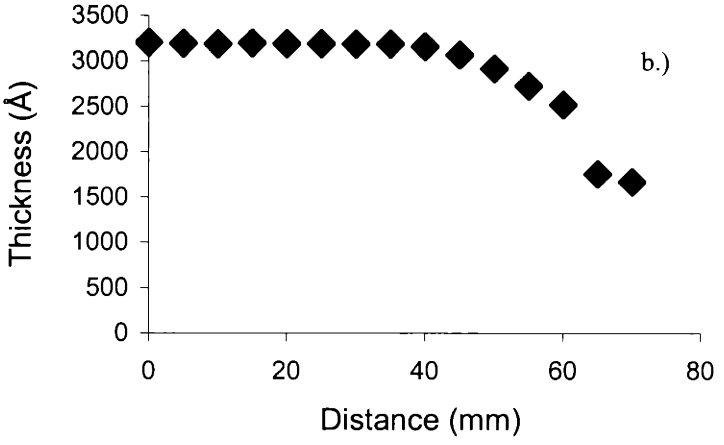

b.)

Figures 4.8a and b: Demonstrating the ability to create a gradient in etching PAA/.PAH multilayer films using NaCl. 4.8a shows a silicon substrate that was dipped in a solution containing a concentration gradient of NaCl while 4.8b shows thickness measurements at incremental distances along the axis of the gradient.

This technique could be combined with anti-reflection coatings developed from these films to be used in optical communications to tailor the light in optical switches.

4.5. Chapter 4: Conclusion

A new method of patterning ionically bonded polyelectrolye multilayer films has been demonstrated using salt solutions, and gives etching control on the nanometer scale. The technique is demonstrated using PAA (3.5)/PAH (7.5) films, as they are useful in anti-reflection coatings and have thick individual bilayers, but the etching phenomenon is shown to not be limited to this specific polymer system. It is also shown to work whether the surface layer is the polycation or the polyanion, although the extent to which the film

is etched differs. Salts of higher ionic strength etch the films more strongly, showing that better thickness control can be attained using a monovalent salt rather than a divalent one.

It can be concluded that the etching mechanism in these films is a combination of layer dissolution from the film and film microstructure rearrangement. It is known that salt ions interact with the polyelectrolytes to shield their charges during film formation and thus can increase film solubility during dissolution [3]. However, this is not the only effect at work in this case because a film that has been etched by a solution of high molarity cannot be further etched by submerging it into a bath of lower molarity. Thus the surface structure of the film must rearrange during the etching process.

These patterned films can be used on reflective substrates to form varied color reflectors, or on transparent conducting substrates in conjunction with spin-cast $Ru(bpy)_3$ films in light-emitting electrochemical cells, as described in chapter 3.

References:

[1] Slinker, Bernards, Houston, Abruna, Bernhard, and Malliaras. "Solid-state electroluminescent devices based on transition metal complexes". *Chem. Commun.* 2003: 2392-2399.

[2] Shiratori, Rubner. "pH-Dependent Thickness Behavior of Sequentially Adsorbed Layers of Weak Polyelectrolytes". *Macromolecules* 2000, 33: 4213-4219.

[3] Dubas, Schlenoff. "Polyelectrolyte Multilayers Containing a Weak Polyacid: Construction and Deconstruction" *Macromolecules* 2001, 34: 3736-3740.

[4] Berg MC, Choi J, Hammond PT, and Rubner MF. "Tailored micropatterns through weal: Polyelectrolyte stamping". *Langmuir* 19 (6): 2231-2237. 2003

[5] Hiller J, Mendelsohn JD, Rubner MF "Reversibly erasable nanoporous anti-reflection coatings from polyelectrolyte multilayers." *Nature Materials* 1 (1): 59-63 2002

[6] Choi, J and Rubner, M.F. Unpublished data.

5. Thesis Conclusion

In this work, various aspects of $Ru(bpy)_3$ light-emitting electrochemical cells were explored, from fabrication in chapter 2, to property improvement in chapter 3, to patterning for applications in chapter 4. In conjunction with this, some properties and uses of polyelectrolyte multilayer films were investigated.

The work in chapter 2 demonstrated the possibility of creating LEC's by loading $Ru(bpy)_3^{2+}$ cations into films of poly(acrylic acid) and poly(acrylamide). These devices were fabricated using only water-based solutions, and have the possibility of being produced over large areas. Unfortunately, the device characteristics such as turn-on voltage, luminance, and stability are not comparable to the device characteristics of spun films, making them unsuitable for practical applications.

The devices in chapter 3 show progress in moving $Ru(bpy)_3$ LEC's toward their being used in practical applications. Blending the spin cast films with polymers makes the devices more stable. Certain polymers such as PC and PMMA, which have hydrophilic groups, show large ion mobility in the films and have very fast response times and efficiencies of 1.75-2.25%. Other polymers such as PS and PVK are completely hydrophobic and have slower response times, but have efficiencies between 2.7 and 3.0% and much longer lifetimes. Another reason for the increased device performance in PS and PVK could be due to their aromatic side groups that could assist in the charge transport that enables these devices to emit light. Thus the structure of the polymer in the blend has an effect on the properties of the device.

Chapter 4 explored a method of patterning multilayer films to be used in conjunction with the $Ru(bpy)_3$ LEC's in order to create patterned emitters. Insulating films fabricated from ionically bonded multilayers of PAA and PAH were etched using aqueous salt solutions at neutral pH to give controlled thicknesses on the nanoscale. This etching method is independent of the specific polymer system – it is effective on any ionically bonded multilayer film. It is dependent on ionic strength, as higher ionic strength solutions etch the films more quickly and effectively, and lower ionic strengths give higher resolution control over thickness. This technique has the interesting property of non-cumulative etching: if a film is etched using a high molarity salt it cannot be further etched using a lower molarity salt. This shows that the salt etching not only dissolves layers away from the film, it rearranges the surface, making further etching impossible. This technique has applications that can extend to any process in which ionically bonded polyeletrolyte are used – in the fields of biomaterials, photonic materials, or electronic materials – in addition to being useful for patterning $Ru(bpy)_3$ LEC's.

In conclusion, light-emitting electrochemical cells based on the $Ru(bpy)_3$ transition metal complex are very attractive candidates to be used in future display applications. The work in this thesis explored various aspects of these devices, and with further research, these LEC's could become widespread in commercial appliances in the near future.